Effect of Wind Shear and Ground Plane on Aircraft Wake Vortices

M.R. Brashears,* N.A. Logan,†
Lockheed Missiles & Space Company, Inc., Huntsville, Ala.

and

James N. Hallock‡
DOT/Transportation Systems Center, Cambridge, Mass.

A previous comparison of predicted wake vortex transport with experiment revealed two consistent sources of discrepancy, namely, lower predicted sink rates of the vortex pair relative to observed and a lagging of the predicted upwind vortex transport compared with the measured values. It was hypothesized that either a wake tilting or a decrease in circulation was occurring to account for this lagging. Accordingly, an analysis was performed to determine the streamlines associated with the presence of a vortex pair in a shear near the ground and the movement of the stagnation points in such a region. It was found that the upper and lower stagnation points rise or sink relative to their shearless location, depending upon the magnitude of nondimensional parameters defining ground proximity and wind shear to circulation.

I. Introduction

To understand more fully the mechanisms involved in aircraft wake tilting, that is, that of the upwind or downwind vortex rising relative to work other vortex, an analysis was performed to determine the streamlines associated with the presence of a vortex pair near a ground plane; the vortex pair is assumed to be acted upon by a wind shear (i.e., the velocity in the horizontal direction is a function of the altitude above the ground plane). The case of a vortex pair in which the individual vortices possess arbitrary circulation (i.e., the circulation is not assumed to be equal and opposite) and located at unequal heights was considered and formulated. However, due to the large number of parameters involved, it was deemed advisable to keep the initial study confined to the simpler case of a pair of vortices possessing equal and opposite circulation Γ and located at equal heights above the ground plane. The special case of the vortex pair at "infinite" distance above the ground plane has already been considered.[1] In the present work, however, a closed form solution was obtained for the special case of the absence of ground effect.

II. Formulation

The defining mathematical equations are relatively simple. Streamlines are to be calculated with respect to a coordinate system which has its x-axis passing through the centers of the vortex pair; the coordinate system will move with the vortex pair (e.g., as it descends and moves horizontally). Let the vortices be separated by a distance $2a$ and let the vortices be at a height b above the ground plane. The mutual attraction of the vortex pair and the image vortex pair will result in a settling motion (neglecting any buoyancy effects) given by

$$V_s = (\Gamma/4\pi a)\ (b^2/a^2+b^2)$$

Presented as Paper No. 74-506 at the AIAA 7th Fluid and Plasma Dynamics Conference, Palo Alto, Calif., June 17-19, 1974; submitted October 29, 1974; revision received January 9, 1975.

Index category: Jets, Wakes, and Viscid-Inviscid Flow Interactions.

*Program Manager Wake Vortex Program. Member AIAA.

†Staff Scientist, Remote Sensing Group.

‡Developmental Engineer, Wake Vortex Program. Member AIAA.

It is assumed that the horizontal wind is described by $U(h)$, where $h=b+y$ denotes the height above the ground plane. The coordinate system moves horizontally with the velocity $U(b)$ and descends vertically with the velocity V_s. The geometry is depicted in Fig. 1.

The stream function for the flowfield in the moving coordinate system is

$$\psi(x,y) = \int_0^y [U(y'+b)]dy' - \frac{\Gamma}{4\pi a}\ \frac{b^2}{a^2+b^2}x$$

$$-\frac{\Gamma}{4\pi}\ln\frac{[(x-a)^2+y^2]\ [(x+a)^2+(y+2b)^2]}{[(x+a)^2+y^2]\ [(x-a)^2+(y+2b)^2]}$$

The velocities are determined by the equations

$$u(x,y) = \partial\psi(x,y)/\partial y \quad v(x,y) = -\partial\psi(x,y)/\partial x$$

To present graphical presentations of the streamlines, it will be convenient to introduce the dimensionless coordinates

$$x'=x/a \quad y'=y/a \quad \epsilon=b/a \quad \psi'(x,y) = (4\pi/\Gamma)\psi(x,y)$$

and it will be advantageous to consider the special case for which $U(h)$ can be represented in the form

$$U(h) = K_0 + K_1(h-b) + K_2(h-b)^2 + \ldots.$$

where terms involving $K_2, K_3, \ldots$ can be neglected to allow superpositioning of the shear and vortex flow.

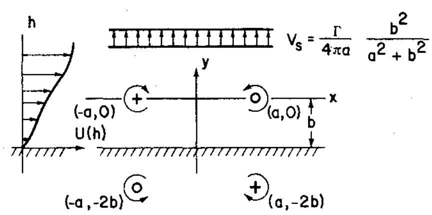

Fig. 1 Coordinate system and flow geometry for vortex pair in wind shear above a ground plane.

This permits the use of the simplification

$$\int_0^y [U(y^*+b)-U(b)]dy^* \simeq$$

$$\int_0^y K_1 y^* dy^* = \tfrac{1}{2}K_1 y^2 = \tfrac{1}{2}K_1 a^2 y'^2 = \frac{\Gamma}{4\pi}\sigma y'^2$$

where

$$\sigma = 2\pi K_1 a^2/\Gamma$$

Suppressing the "primes"

$$\psi(x,y) = y^2\left[\frac{\epsilon^2}{1+\epsilon^2}\right]x - \ln\left\{\frac{[(x-1)^2+y^2]\,[(x+1)^2+(y+2\epsilon)^2]}{[(x+1)^2+y^2]\,[(x-1)^2+(y+2\epsilon)^2]}\right\}$$

$$= f_1(x,y;\sigma,\epsilon)$$

$$u(x,y) = f_2(x,y;\sigma,\epsilon)$$

$$= 2\sigma y - \left\{\frac{8xy}{[(x-1)^2+y^2]\,[(x+1)^2+y^2]}\right\} - \frac{8x(y+2\epsilon)}{[(x-1)^2+(y+2\epsilon)^2]\,[(x+1)^2+(y+2\epsilon)^2]}$$

$$v(x,y) = f_3(x,y;\sigma,\epsilon)$$

$$= \frac{\epsilon^2}{1+\epsilon^2} + \frac{4[(x^2-1)-y^2]}{[(x-1)^2+y^2]\,[(x+1)^2+y^2]} - \frac{4[(x^2-1)-(y+2\epsilon)^2]}{[(x-1)^2+(y+2\epsilon)^2]\,[(x+1)^2+(y+2\epsilon)^2]}$$

III. Solution

The equations for the streamlines can be generated by integration of the differential equation

$$\frac{dy(x)}{dx} = \frac{v(x,y)}{u(x,y)} = f_3(x,y;\sigma,\epsilon)/f_2(x,y;\sigma,\epsilon)$$

between x and $x+dx$ when $|dy/dx|<1$, by integration of

$$\frac{dx(y)}{dy} = \frac{u(x,y)}{v(x,y)} = f_2(x,y;\sigma,\epsilon)/f_3(x,y;\sigma,\epsilon)$$

between y and $y+dy$ when $|dx/dy|<1$.

The numerical integration will break down when $u(x,y)$ and $v(x,y)$ vanish simultaneously at a stagnation point (x^*, y^*). Therefore, it is important to determine in advance the location of the streamline $f_1(x^*,y^*;\sigma,\epsilon)=f^*$ which passes through the stagnation point (x^*,y^*). This requires the determination of (x^*,y^*) by solving the set of simultaneous equations

$$u(x^*,y^*)=0 \quad v(x^*,y^*)=0$$

It is proposed that this pair of values (x^*,y^*) be determined by an iterative solution

$$x_{n+1} = x_n - [A_{22}u(x_n,y_n) - A_{12}v(x_n,y_n)]/\Delta$$

$$y_{n+1} = y_n - [A_{11}v(x_n,y_n) - A_{21}u(x_n,y_n)]/\Delta$$

where

$$\Delta = A_{22}A_{11} - A_{12}A_{21} = A_{11}A_{22} - A_{21}A_{12}$$

and

$$A_{11} = [u(x_n+\tfrac{1}{2}\delta,y_n) - u(x_n-\tfrac{1}{2}\delta,y_n)]/\delta$$

$$A_{12} = [u(x_n,y_n+\tfrac{1}{2}\delta) - u(x_n,y_n-\tfrac{1}{2}\delta)]/\delta$$

$$A_{21} = [v(x_n+\tfrac{1}{2}\delta,y_n) - v(x_n-\tfrac{1}{2}\delta,y_n)]/\delta$$

$$A_{22} = [v(x_n,y_n+\tfrac{1}{2}\delta) - v(x_n,y_n-\tfrac{1}{2}\delta)]/\delta$$

The starting values for the iteration will be selected by determining the values of (x^*,y^*) for the simpler case in which $\epsilon\to\infty$; i.e., the case in which the effect of the image vortex in the ground plane can be neglected. This problem involves the somewhat simpler problem defined by solving for (x,y)

$$0 = 2\sigma y - \left\{\frac{8xy}{[(x-1)^2+y^2][(x+1)^2+y^2]}\right\}$$

$$0 = 1 + \left\{\frac{4[(x^2-1)-y^2]}{[(x-1)^2+y^2][(x+1)^2+y^2]}\right\}$$

These equations can be used to show that

$$y^2 = x^2 - 1 + x/\sigma$$

The value of x can be determined from the equation

$$(x+1/2\sigma)^2 = 1 + 1/\sigma x$$

which is a cubic equation of the form

$$x^3 + px^2 + qx + r = 0$$

with

$$p = 1/\sigma \quad q = 1/4\sigma^2, \quad r = -1/\sigma$$

The solution can be expressed in the form

$$x = z - \tfrac{1}{3}p = z - 1/3\sigma$$

where z is a solution of the cubic equation

$$z^3 + az + b = 0$$

where

$$b = -(72\sigma^2+1)/108\sigma^2 \quad a = -(12\sigma^2+1)/12\sigma^2$$

The nature of the roots is determined by the factor

$$Q = (b^2/4) + (a^3/27) = (1+44\sigma^2-16\sigma^4)/432\sigma^4$$

This expression vanishes at $\sigma_c = \pm 1.665095388$ $[\sigma_c^2 = (11+(125)^{1/2})/8 = 2.772542486]$. From the theory of cubic equations it follows that x has one real root for $0<\sigma<\sigma_c$; three real roots (two equal) for $\sigma=\sigma_c$; and three real roots (all different for $\sigma>\sigma_c$. For $0>\sigma>\sigma_c$ the real root is given by

$$x = (P+R)^{1/3} + P^{1/3} - R - 1/3\sigma$$

where

$$P = (72\sigma^2+1)/216\sigma^3 \quad R = \sqrt{Q}$$

For $\sigma=\sigma_c$ the real roots are given by

$$x_1 = 2(P)^{1/3} - 1/3\sigma = 0.9717365426$$

$$x_2 = x_3{}^* - \tfrac{1}{2}x_1 = -0.485868271$$

For $\sigma > \sigma_c$ the three distinct real roots are given by

$$x_1 = A\cos(\theta) - 1/(3\sigma)$$

$$x_2 = A\cos(\theta + 2\pi/3) - 1/(3\sigma)$$

$$x_3 = A\cos(\theta - 2\pi/3) - 1/(3\sigma)$$

where

$$A = 1/(3\sigma)(12\sigma^2+1)^{1/2} \quad \cos(3\theta)$$

$$= \frac{1}{(12\sigma^2+1)^{1/2}} \quad \frac{72\sigma^2+1}{12\sigma^2+1}$$

The angle θ is 0 for $\sigma = \sigma_c$. for $\sigma \to \infty$

$$\theta \simeq (\pi/6) - 1/3(72\sigma^2+1)/[12\sigma^2+1]^{3/2}$$

The only positive root is x_1. We observe that $\sigma = \sigma_c$, the value calculated from $x = A \cos \theta - 1/3\sigma$ yields $x = 0.9717365426$ for $\sigma = \sigma_c$; this agrees with the value obtained from the expression

$$x = 2P^{1/3} - 1/(3\sigma)$$

which is the limiting case of

$$x = (P+R)^{1/3} + (P-R)^{1/3} - 1/(3\sigma) \quad \text{as} \quad \sigma \to \sigma_c$$

from below. We observe that $x \to 0$ as $\sigma \to 0$

since

$$(P \pm R)^{1/3} \to 1/(6\sigma)$$

The previous equations completely define the value of x in terms of the parameter σ. The corresponding values of y are determined from $y^2 = x^2 - 1 + x/\sigma$. We observe that, for $\sigma \to 0$, $x \to 4\sigma$; therefore

$$y \to \pm\sqrt{3} \quad \text{as} \quad \sigma \to 0$$

These values provide a set of starting values for the more general case in which $\epsilon = b/a$ is finite. Note that if the wind shear cannot be expressed analytically in the form $U(h) = U(b) + K_1(h-b)$, then one can obtain an approximate value of K_1 by means of $K_1 = [U(b+\delta) - U(b)]/\delta$ and therefore take σ to be defined by

$$\sigma = 2\pi[U(b+\delta) - U(b)a^2/\delta\Gamma$$

Observing that when $\sigma \to 0$, then the previous initial values for the stagnation points are undefined. In this limiting case, $x = 0$ and $y = \pm\sqrt{3}$.

Experience with the previous iterative formula for the roots for the case $\epsilon \neq \infty$ revealed that the starting values obtained for the case of $\epsilon = \infty$ leads to numerical problems as $\epsilon \to 0$. This was "fixed" in the analysis by observing that the stagnation point nearest the ground plane has the approximate values $x = x^*$ and $y = -\epsilon$, where x^* is a solution of the equation $8x = \sigma(x^2-1)^2$. In practice it was found that a very satisfactory numerical problem was defined by merely setting $x = 1/2$ and $y = -\epsilon$ where ϵ was less than 0.7. It was also found useful to employ the results

$$x \simeq (4\sigma) - (4\sigma)^3 + 0.75(4\sigma)^5 \qquad y \simeq 3 - 3(4\sigma)^2 + (4\sigma)^4$$

for starting values (i.e., the results for $\epsilon \to \infty$) when σ tends toward 0.

IV. Analysis

Figure 2 provides a chart for which the coordinate (x,y) of the upper and lower stagnation points can be determined for any set of values of wind shear and ground plane proximity. Note that the values of y for the lower stagnation point are the absolute values of the actual coordinates. This graphic presentation of the roots (which yield the upper and lower stagnation points) indicates that under certain circumstances the upper stagnation point will rise rather drastically. This occurs for small values of σ as ϵ tends toward zero. Therefore, this effect occurs under the condition of a small wind shear (or large circulation) as the vortex pair descends toward the ground. This is seen to occur for all σ values other than 0.5 (actually some value between 0.3 and 0.5, but only these two discrete values are shown on the graph) as ϵ decreases in value from infinity. If the aircraft altitude is finite, which is certainly the case, the intersection of the initial altitude relative to the semispan and the wind shear curves locates the initial point on the plot. For commercial jet aircraft outside the threshold, ϵ is approximately unity initially; thus the downwind upper stagnation point will rise for σ less than 0.3 (corresponding figures for the middle marker are $\epsilon \sim 4.0$ and $\sigma < 4.0$).

Figures 3-5 show the detailed streamlines for various values of ϵ corresponding to a heavy shear ($\sigma = 3.0$). Note the downwind vortex cell is strikingly smaller than the upwind cell (this was previously reported[1] for the special case of $\epsilon \to \infty$). Note also that the upper and lower stagnation points are on different streamlines. This gives rise to a streamtube between the stagnation streamlines and the steady-state case allows a "sweeping" motion of fluid in the external stream from the lower right around the upwind cell, back around the downwind cell and exiting via the upper right. In the actual case, this idealistic steady-state situation does not exist. However, as the oval sinks, the tendency would be for a detrainment of the upwind fluid to occur with the size of the streamtube increasing with decreasing ϵ as shown in Figs. 3-5.

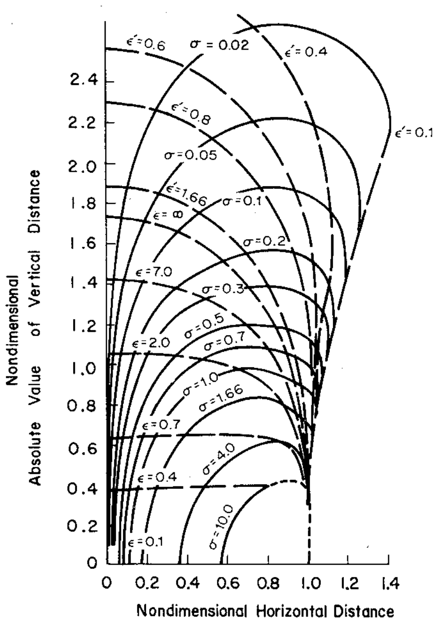

Fig. 2 Location of stagnation points on vortex oval as a function of wind shear and proximity of ground plane (ϵ' refers to upper stagnation point, ϵ to lower).

V. Additional Thoughts on Mechanism of Wake Tilting

Previously, it was hypothesized that wind shear might correlate with wake tilting. A slight trend was observed for the upwind vortex to rise in a heavy shear while the downwind vortex appeared to rise in a slight shear. Consider the data plotted in Fig. 6. This represents the maximum difference in altitude between the downwind and upwind vortices (Δh max/$\bar{h}$ positive means the downwind vortex is higher than the

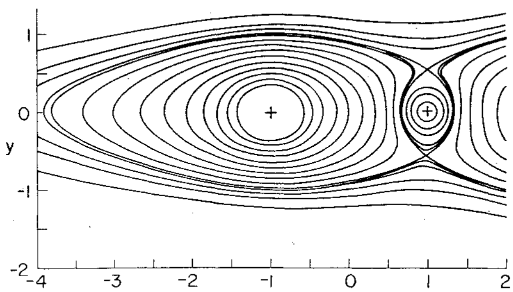

Fig. 3 Streamlines for $\sigma = 3.0$, $\epsilon = 2.0$.

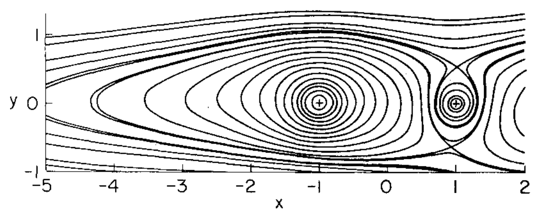

Fig. 4 Streamlines for $\sigma = 3.0$, $\epsilon = 1.0$.

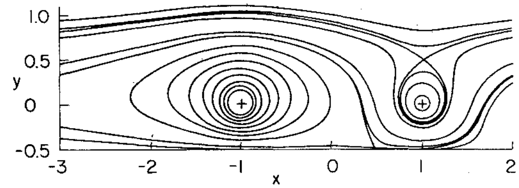

Fig. 5 Streamlines for $\sigma = 3.0$, $\epsilon = 0.5$.

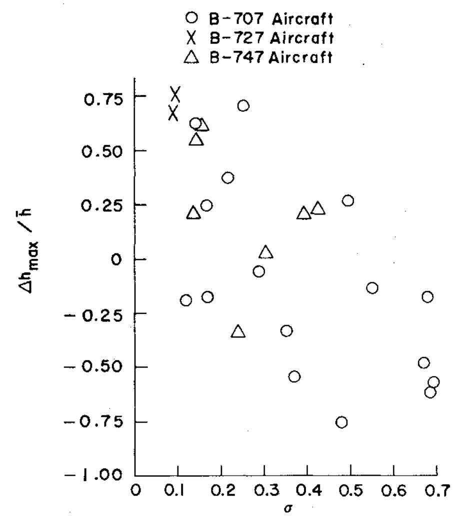

Fig. 6 Vortex altitude mismatch vs sigma.

upwind) as a function of σ. There is a definite trend for the upwind vortex to be at a higher altitude for large shears and for the downwind vortex to be higher in light shear. Also note the crossover point occurs at a σ of 0.3-0.4. The flybys were made with the aircraft at a 175-ft altitude ± 30 ft, which defines the initial ϵ as roughly 3.0 for the B-747, 4.0 for the B-707, and 5.0 for the B-727. Figure 2 shows the crossover point for these values of ϵ as between $\sigma = 0.3$ and $\sigma = 0.5$. This agrees surprisingly well with the experimental data if it is assumed that the upper stagnation point trend defines which vortex rises.

Observations from the Simplified Theory

In the light shear the upper stagnation rises as the oval descends toward the ground. In a strong shear the upper stagnation moves closer to the ground. Wind shear tends to move the stagnation points downwind.

Ground proximity tends to draw both the stagnation points toward the ground in a strong shear. Ground plane tends to "open up" a region between the two cells and causes a sweeping motion of the external stream around the cells.

The downwind cell gets smaller as wind shear and ground proximity increase. The upwind cell increases in area as wind shear increases and altitude increases.

Possible Implications of These Preliminary Results

The downwind vortex cell shrinkage with increasing wind shear may give rise to an increased detrainment of the vorticity, as the increasing core size will encounter the inviscid cell boundary quicker than in the upwind case. This would cause the upwind vortex to rise due to the decreased induced velocity by the downwind vortex. The sweeping motion might cause upwind cell detrainment, thus causing the downwind vortex to rise.

Even though an extremely limited amount of data is available on wake tilting, the fact remains that the crossover point between upwind and downwind vortex rising based both on the simplified theory and available data cannot be overlooked and should be investigated further. Buoyancy effects may be important, as some increased success was obtained by considering lapse rate in the attempted correlations (see Ref. 2).

References

[1] Lissaman, P.B.S., Crow, S. C., MacCready, P. B., Tombach, I. H., and Bate, Jr., E. R., "Aircraft Vortex Wake Descent and Decay under Real Atmospheric Effects," Rept. FAA-RD-73-120, Oct. 1973, AeroVironment, Inc., Pasadena, Calif.

[2] Brashears, M. R., Logan, N. A., Robertson, S. J., Shrider, K. R., and Walters, C. D., "Analysis of Predicted Aircraft Wake Vortex Transport and Comparison with Experiment," Rept. FAA-RD-74-74.I, April 1974, Lockheed Missiles & Space Co., Huntsville, Ala.